

Withdrawal through non-rectangular channels

By A. Odulo and J.C. Swanson

Abstract: Withdrawal of a homogeneous inviscid fluid from a large basin into an empty large basin through a constriction, whose slope and cross-sectional area vary in an arbitrary manner, is considered. Geometrical and algebraic methods to find the water discharge are presented.

Analytical solutions for particular channels, whose width varies with both depth and along channel distance, and where the sill and the narrows do not coincide, are found. They illustrate the influence of the channel geometry on the discharge, the position of the critical point, and the water velocity at the critical point. The theory allows us to predict the withdrawal discharge through natural constrictions and to design constrictions with specific withdrawal properties.

The theory is also valid for salt-water withdrawal into a basin with fresh water (reduced gravity model), if the free surface is flat and, as result, the upper layer is motionless. It gives an upper limit for the discharge of the denser fluid in the case of a two-layer exchange flow. Also presented is the solution for a lighter fluid run up over a stationary denser layer, which gives an upper limit for the discharge of the lighter fluid in the case of a two-layer exchange flow.

Solution for one layer flow gives particular solutions for a multi-layer flow as well.

Keywords: withdrawal; non- rectangular channel; critical point

1.Introduction

The determination of the discharge of a fluid flowing through a constriction is relevant to many engineering activities (Bakhmeteff 1932; Chow 1959; Ackers *et al.*, 1978). It is also important for understanding and predicting flows through constrictions in estuaries and through straits (Bormans & Garrett 1989; Dalziel 1992; Baines, 1995, Pawlak & Armi 1997).

Ackers *et al.* (1978), as did the authors of most of the previous works, considered channels in which the sill and the narrows coincide. In this case the along channel geometry has no influence on the discharge, the position of the critical section is known a priori and the solution can be found in textbooks (i.e. Chow, 1959, § 3-3). In natural channels the position of the narrowest section does not usually coincide with the position of the sill, nor the shape of the cross-section is unvaried along the channel. In this case, the analysis of flow becomes difficult because the position of the critical point is part of the problem and its position cannot be determined easily. We shall show that the wrong choice of the critical point can lead to significant error in the prediction of the discharge. For similar cross-section channels (see §3 below) the position of the critical point depends only on the along channel geometry and can be found as discussed in Gill (1977, §2).

Wood (1968, 1978), Wood & Lai (1972) dealt with the case of withdrawal of the two-layer fluid through a rectangular section channel.

The withdrawal of homogenous fluid from a large basin is a particular case of an exchange flow between two large basins with fresh and salt water (see Appendix). Exchange flows through a rectangular channel were intensively studied (Wood 1970, Baines 1995, § 3.11). The analytical solution for a rectangular channel was obtained for exchange flow through a contraction (Odulo *et al.* 1997a) and over a sill (Odulo *et al.* 1997b). Odulo & Swanson (1998) considered an exchange flow through a rectangular channel, whose width and depth vary along the channel in an arbitrary manner. Dalziel (1992) studied the exchange of a two-layer flow through a constriction with a non-rectangular section. For parabolic cross-section he calculated the layer discharges and presented analytical results for the limits when one or the other layer was brought to rest. Bormans & Garrett (1989) provided numerical calculations, which showed that “using triangular instead of rectangular cross-section raises the interface everywhere along the strait”.

In this paper withdrawal from a basin filled with a homogeneous inviscid fluid into an empty basin (or into a basin filled lighter fluid with the same level) through a constriction, whose slope and cross-sectional

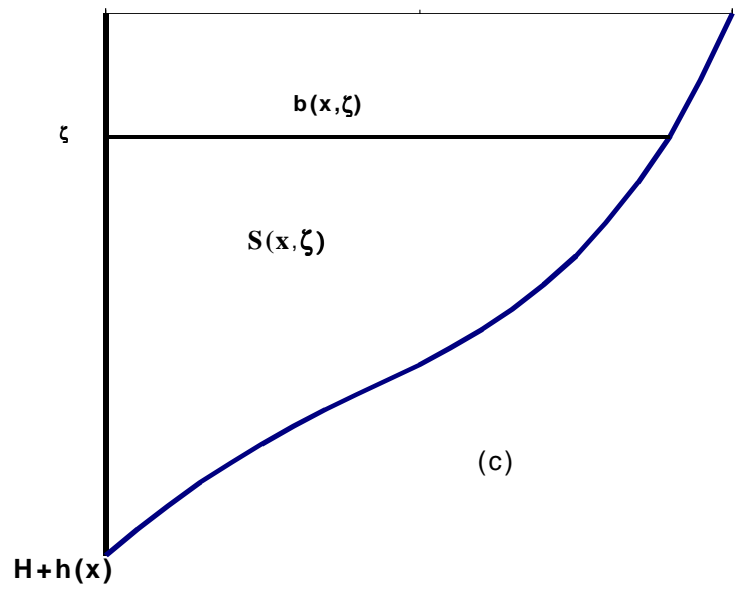
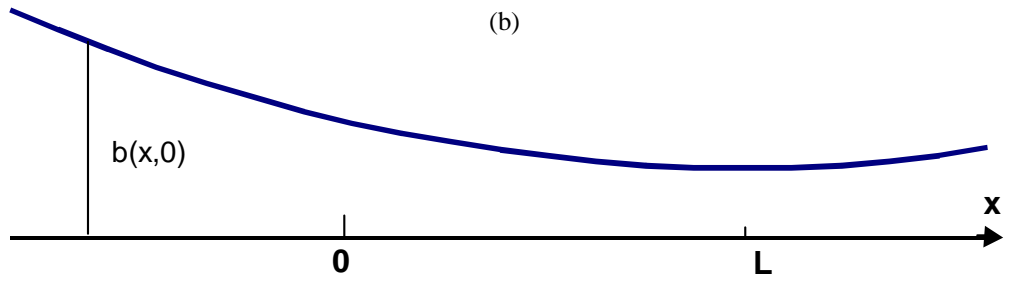
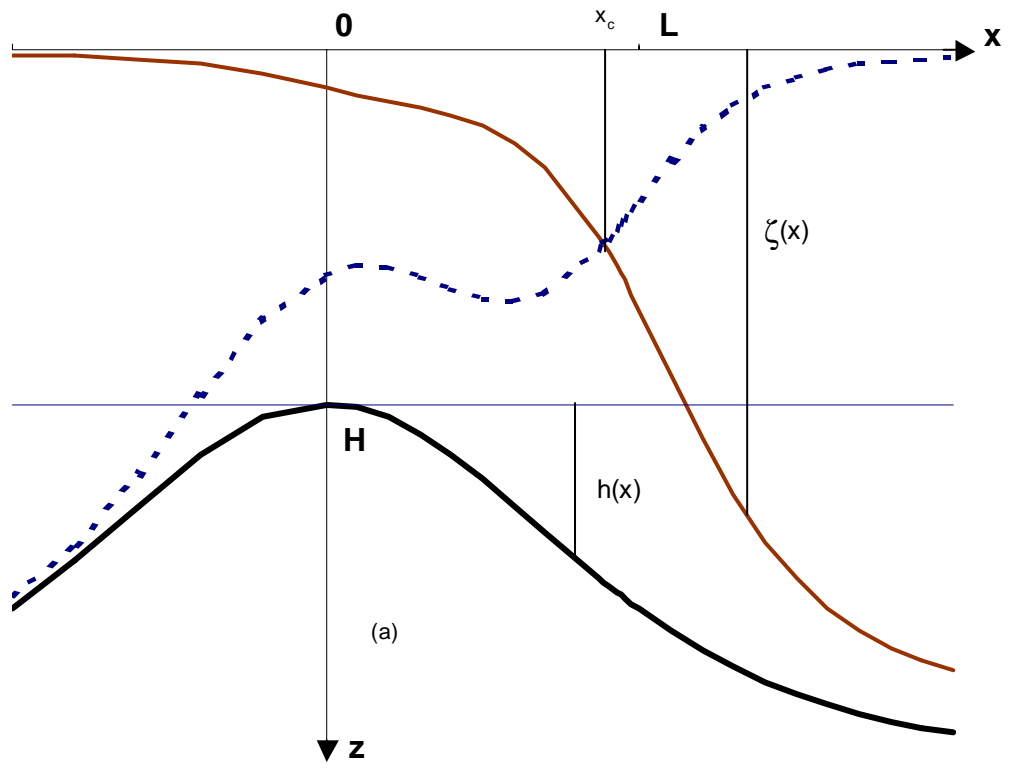


Figure 1 (a) Side view of flow through a constriction with geometry $h(x)=H \tanh^2(5x/4)$ and $b(x,0)=b_0[4-3/e^{(x-1)^2}]$ in the region $-1 < x < 2$; $b(x)$ infinitely increases at $x \rightarrow \pm\infty$. The solid line shows the water surface for a withdrawal from the left basin, the dash line for a withdrawal from the right basin. Calculations were made using (3.17). (b) Top view of the channel at the level $z=0$. (c) Scheme of channel cross-section.

area vary in an arbitrary manner, is considered. The basin width is infinitely large far from the constriction. A channel depth has a minimum at a position, called a bottom crest (or sill), and increases with distance from it (figure 1a). The channel width changes along a channel (figure 1b) and with depth (figure 1c). Generally, at different depths the channel has a minimum width at different positions along the channel (see example in §5 below). We define as the narrows the most distant position of such minimum widths from the crest, and denote the distance between the crest and the narrows as L .

The x -axis points along the channel from the bottom crest to the narrows. The z -axis points vertically downwards. The origin is at the level of the fluid in the basin and located above the bottom crest (figure 1a). The basin cross-section area $S(x,z)$ is infinitely large far from the constriction.

It is important to point out the difference between a free outflow from a large basin and a flow initiated by a towed obstacle in a prismatic channel (Baines 1995) or a jet running over an obstacle (Ohtsu *et al.* 1996). In the latter cases the speed of the fluid relative to the obstacle can be arbitrary. Depending on upstream and downstream conditions and the obstacle size, different regimes are possible (e.g. figure 2.11 in Baines 1995, and figure 1-2 in Ohtsu *et al.* 1996). If a steady regime can be achieved (in the system coordinates moving with an obstacle in the case of a towed obstacle), the discharge (the volume flux) Q is the product of the towed obstacle velocity (or the jet velocity) and the fluid section far upstream. The discharge does not depend on the geometry of the obstacle. In the withdrawal case, the discharge depends only on the channel geometry and the water surface level in the basin measured from the bottom crest

datum, H . The fluid velocity at the bottom crest cannot exceed $(2gH)^{1/2}$. So we have a very rough estimation of the discharge: $Q < (2gH)^{1/2} S_0$. Here S_0 is the flow area at the bottom crest.

The mass conservation law

$$S(x, \zeta)u(x) = Q \quad (1.1)$$

can be considered as the definition of the average velocity of the flow, $u(x)$. Here $S(x, \zeta)$ is the fluid cross-section area (figure 1c), $\zeta(x)$ is the water surface drop from the upstream water level (figure 1a) and Q is the discharge (which is constant for steady flow). It is convenient to use the water surface drop, ζ , as the dependent variable instead of the water depth. The second equation we use is the Bernoulli equation (Chow 1959, p.40)

$$u^2 = 2g\zeta. \quad (1.2)$$

Here g is the gravitational acceleration (in the case of a withdrawal into an empty basin) or the reduced gravitational acceleration (in the case of flow of salt water into a fresh water basin with the same level). In the latter case ζ is the depth of the interface. It is common to use the mass conservation and Bernoulli's laws for steady flows in open channels (e.g. Baines, 1995, Eq. (2.3.40)-(2.3.41)). However, the solutions for channels, whose cross-section area shapes vary along the channel, and the bottom crest and the narrow do not coincide, are found in this paper for the first time.

If $u(x)$ is an average velocity defined by (1.1), then (1.2) is an approximation. The Bernoulli equation (1.2) is valid under assumptions that the vertical and cross channel components of the velocity are much smaller than the along channel component, the velocity is uniform over the channel section and that friction is negligible. Real flows are three-dimensional and frictional. Therefore, the disagreement between the experimental values and the theoretical ones always exists, unless the errors in measurements compensate for it. Introducing empirical correction coefficients can minimize disagreement between the predictions and experimental data (Ackers *et al.* 1978). The empirical correction coefficient is useful for practical purposes, but does not clarify the physics, because it takes account of all neglected effects combined.

Equations (1.1) and (1.2) contain two unknown functions, $u(x)$ and $\zeta(x)$, and unknown discharge Q . To solve the problem, one more condition is required. The obvious requirement is decreasing the water depth to 0 in an infinitely wide basin downstream. It will be shown in § 3.3 that the continuous solutions do not exist for some channel cross-sections.

Far upstream, the water surface drop and water velocity are zero. One can say that (1.2) describes the transformation of potential energy into kinetic energy.

Many authors have discussed the influence of friction on flow by adding to the Bernoulli equation (1.2) a frictional term (e.g. Baines 1995, Eq. (2.3.57)). Such a parameterization of friction was successfully used for flows in channels with a sloped bottom. For the withdrawal problem, it is preferable to use “the effective flow area” concept (Wood 1970, p. 673; Ackers *et al.* 1978, Eq. (2. 10) p. 36) or to use the correction coefficients (Ackers *et al.* 1978, Eq. (8.9), p 171).

The purpose of this paper is to determine the withdrawal discharge of one-layer flow through a non-prismatic channel of variable slope.

2. General solution

(a) Equation for the water surface profile

Consider steady free outflow from a large basin through a channel whose width, $b(x,z/(H+h(x)))$, varies with both depth (figure 1c) and along channel distance (figure 1b). The water cross-section area is (figure 1c)

$$S(x,\zeta)= \int_{\zeta}^{H+h(x)} b(x, z/(H + h(x)))dz . \quad (2.1)$$

Here $h(x)$ is the depth of the lowest point of the channel section measured from the bottom crest level. The bottom crest is at $x=0$, $h(0)=0$ (figure 1a).

Eliminating u from (1.1)-(1.2) we get

$$\zeta^{1/2}S(x, \zeta)=Q/(2g)^{1/2}. \quad (2.2)$$

For a given geometry ($H+h(x)$, $b(x,z)$), this equation determines the water surface profile $\zeta(x)$. Here $z = z/(H+h(x))$.

The problem is to determine the discharge Q such that $\zeta(x)$ changes continuously in the flow direction from the upstream value 0 to the downstream value $H+h(\infty)$ for a flow from the left basin, or to the downstream value $H+h(-\infty)$ for a flow from the right basin.

(b) Geometrical solution.

Denote the right side of the equation (2.2) as $F(x,\zeta)$

$$F(x,\zeta) = \zeta^{1/2} S(x,\zeta). \quad (2.3)$$

One can call $F(x,\zeta)$ the specific discharge surface by analogy to the specific energy curve [figure 30 in Bakhmeteff (1932); figure 3-2 in Chow (1959)]. This function is determined in the domain $-\infty < x < \infty$, $0 \leq \zeta \leq H+h(x)$. It is equal to 0 at $\zeta = H+h(x)$ (see (2.1)) and at $\zeta = 0$, $F(x, H+h(x)) = F(x, 0) = 0$, and infinitely increases far upstream and downstream, $F(-\infty, \zeta) \rightarrow \infty$, $F(\infty, \zeta) \rightarrow \infty$. Thus, if the surface $F(x,\zeta)$ has a unique critical point (x_c, ζ_c) , then (x_c, ζ_c) is a saddle point. Equation (2.2) has a continuous solution $\zeta(x)$, which changes from 0 to $H+h(\infty)$ [or $H+h(-\infty)$] in the flow direction, only if

$$Q = (2g)^{1/2} F(x_c, \zeta_c). \quad (2.4)$$

If Q is larger than $(2g)^{1/2} F(x_c, \zeta_c)$, then equation (2.2) has no solution in the neighborhood of x_c . If Q is less than $(2g)^{1/2} F(x_c, \zeta_c)$, then equation (2.2) has two solutions. One of them tends to 0 far upstream and downstream, $\zeta(x) \rightarrow 0$ when $x \rightarrow \pm\infty$; the other tends to $H+h(x)$ far upstream and downstream, $\zeta(x) \rightarrow H+h(\pm\infty)$ when $x \rightarrow \pm\infty$. Neither solution has physical meaning for the problem considered here.

The intersection of the plane $y = F(x_c, \zeta_c)$ with the surface $y = F(x, \zeta)$ forms two curves intersecting at the saddle. The projection of these curves on the x, ζ plane (called level curves or contour lines) gives the solution for a flow from the right basin (dashed line in figure 1a), and the solution for a flow from the left basin (solid line in figure 1a).

Note that the water surface has a different shape for the flow in the direction from the bottom crest to the narrows compared with flow from the narrows to the bottom crest.

For an arbitrary channel geometry one can find the critical point of function $F(x, \zeta)$ by drawing a family of level curves (contour lines) to find two curves, which intersect at the saddle. The value of $F(x, \zeta)$ at the saddle multiplied by $(2g)^{1/2}$ gives the discharge (see 2.4). This is the geometrical solution. Compare with Chow (1959), p.p. 46-47, where "non-prismatic channel with variable slope is taken as an example, in which a gradually varied flow is carried from a sub-critical state to a supercritical state (figure 3-5)"

(c) Algebraic solution

To better understand the properties of the flow and the effect of the channel geometry on the flow discharge, we have to find algebraic (preferably analytic) solutions. To simplify the algebra, we represent a channel width as function of x and z' , not x and z , and introduce the relative water surface drop

$$\xi = \zeta / (H + h(x)). \quad (2.5)$$

Then (2.2) takes the form

$$\xi^{1/2} s(x, \xi) (H + h(x))^{3/2} = Q / (2g)^{1/2}. \quad (2.6)$$

Here

$$s(x, \xi) = \int_{\xi}^1 b(x, z') dz'. \quad (2.7)$$

Denote the right side of the equation (2.6) as $F(x, \xi)$

$$F(x, \xi) = \xi^{1/2} s(x, \xi) (H + h(x))^{3/2}. \quad (2.8)$$

We consider this function in the domain $-\infty < x < \infty$, $0 \leq \xi \leq 1$. Obviously, the saddle points of $F(x, \xi)$ and $F(x, \zeta)$ occur at the same positions, x_c , and $\zeta_c = (H + h(x_c)) \xi_c$. The saddle point, (x_c, ξ_c) , of $F(x, \xi)$ is the solution of the system $F_{\xi} = 0$ and $F_x = 0$. This system can be written in the form

$$s(x_c, \xi_c) = 2 \xi_c b(x_c, \xi_c) \quad (2.9)$$

and

$$\int_{\xi_c}^1 S''_x dz' = 0. \quad (2.10)$$

Here $S''(x, z) = (H + h(x))^{3/2} b(x, z)$. The problem is reduced to a system of two algebraic equations (2.9) and (2.10). If we suppose, that this system has a unique solution (x_c, ξ_c) , then solving the system (2.9)-(2.10) we can calculate the discharge

$$Q = (2g)^{1/2} F(x_c, \xi_c). \quad (2.11)$$

Using (2.6), (2.7) and (2.9) one gets

$$F(x_c, \xi_c) = 2\xi_c^{3/2} b(x_c, \xi_c). \quad (2.12)$$

From (2.6) and (2.8) we have $\xi_x = -F_x/F_\xi$. Thus the system (2.9)-(2.10) can be also obtained from the condition that both numerator and denominator of the expression for ξ_x are zero at the same point (x_c, ξ_c) (method of singular points Chow, 1959, § 9-6; Baines, 1995, p. 45-46). We shall show below (§ 3.4) that ξ_x can be 0, finite or infinitely large at the critical point. By definition, the critical point is the point where $F_x = 0$ and $F_\xi = 0$.

Thus, in general, the problem is solved. For any geometry, given analytically or in a table, one can graphically or analytically find the value of $F(x, \xi)$ at a saddle point and then the discharge from (2.11). Below we present analytical solutions for particular geometries to illustrate the dependence of the discharge on the channel geometry.

Equations (2.6), (2.9) and (2.10) correspond to equations (3.1)-(3.3) in Gill (1977). From (2.9) and (2.2) we get the well-known expression for the discharge $Q = (g)^{1/2} Z$ (see Eq. (8.5) in Ackers *et al.* 1978). Here $Z = (S^3(x_c, \xi_c)/b(x_c, \xi_c))^{1/2}$ is the section factor (see Chow 1959, Eq. (2-3) and Table 2-1).

(d) Geometrical interpretation and discussion

Because $S''_x < 0$ for $x < 0$ and $S''_x > 0$ for $x > L$ for all z , it follows from (2.10) that x_c lies between a sill and a narrows. So, to find the critical point we have to know $H + h(x)$ and $b(x, z)$ only between the sill and the narrows. In § 5 we present an example of the channel geometry, for which, at different depths, $S''_x = 0$ at

different positions along the channel. If for all z the width $b(x,z)$ has a minimum at the bottom crest, $L=0$, then the solution of (2.10) is $x_c=0$, and ξ_c is found from (2.9) with $x_c=0$.

Equation (2.9) has a simple geometrical interpretation. At the critical position, x_c , the water surface drop is such that the area of the fluid section, $S(x_c, \zeta_c)$, equals the area of a rectangle with a base equal to the top width, $b(x_c, \xi_c)$, and a height equal to twice the water surface drop, ζ_c .

Introducing the average width of the fluid section area $b_{av}(x, \xi) = s(x, \xi)/(1-\xi)$, we can rewrite (2.9) in the form $\xi_c = \beta/(2+\beta)$, where $\beta = b_{av}(x_c, \xi_c)/b(x_c, \xi_c)$. So, if, at the critical point, the average width of the water area is less than the top width, $\beta < 1$, then the water surface drop is less than one half of the fluid depth, $\xi_c < 1/3$ (in agreement with the conclusion of Bormans and Garrett (1989), p. 1549). Remember, that $\xi_c = 1/3$ for a rectangular cross-section.

We introduce the hydraulic depth D as the ratio of the water area $S(x, \zeta)$ to the top width $b(x, \xi)$, $D = S(x, \zeta)/b(x, \xi)$ (see Chow, 1959, equation (2-2) and Table 2-1). The local Froude number is defined as $Fr^2 = u^2/(gD)$ (Baines (1995), Eq. (2.3.44)). Using (1.2) we get $Fr^2 = 2\xi b/s$. The relative water surface drop ξ increases from 0 upstream to 1 downstream and $s(x, \xi)/b(x, \xi)$ decreases from some value upstream to 0 downstream. Therefore the local Froude number $Fr(x, \xi)$ changes from 0 downstream to infinity upstream. The assumption that ξ , s and b continuously change in the flow direction leads to the conclusion that it must be at least one point x where $Fr=1$. We determined the local Froude number in a such way that it is equal to 1 at the critical point, $Fr(x_c, \xi_c) = 1$ (see Eq. (2.9)). We can equivalently say that at x_c the hydraulic depth is twice the water surface drop, $D = 2\zeta$. This corresponds to the definition of critical flow in Chow (1959), p. 43.

If the values of $S(0, \zeta(0))$, $S(x_c, \zeta(x_c))$ and $S(L, \zeta(L))$ differ significantly, the error in calculation of x_c can lead to a significant error in Q .

(e) Approximation of the channel geometry

Our goal is to predict the discharge through a channel of arbitrary geometry. For natural channels we have to extrapolate from the measured data of the channel geometry. Then we can find the saddle point of the function $F(x, \xi)$ geometrically. Or we can approximate the channel geometry analytically and try to solve the system (2.9)-(2.10). These extrapolations and approximations can be made many different ways. We need criteria for good extrapolations and approximations. Thus we have to understand which characteristics of the geometry influence the value of $F(x_c, \xi_c)$ and, as a result, the discharge Q . Also, we shall approximate the channel geometry in the form, which allow us to solve the system (2.9)-(2.10) analytically.

Only the geometry of the channel between the bottom crest and the narrows influences the discharge. Therefore we have to extrapolate and approximate the channel geometry only in the interval $(0, L)$. This means that it is sufficient to consider the function $F(x', \xi')$ only in the interval $0 < x' < 1$. We denote $x' = x/L$. Further, we shall drop the superscript $'$ over x . Remember that if $L=0$, then $x_c=0$, and the knowledge of $b(0, z')$ is needed only.

If we take $b_0 b(x, z')$ instead $b(x, z')$, the system (2.9)-(2.10) will not change (b_0 is a constant). Therefore, x_c and ξ_c do not depend on b_0 and Q is proportional to b_0 . We can take $b(1, 0)=1$ without losing generality. The system (2.9)-(2.10) can not be solved analytically for arbitrary $b(x, z')$. We limit our study to the approximations of $b(x, z')$ in the form, which includes a wide class of geometries,

$$b(x, z') = b_b(x) + b_1(x)(1-z')^m. \quad (2.13)$$

As before, $z' = z/(H+h(x))$. The geometrical meaning of each term is as follows: $b_b(x)$ describes the change of the bottom width along the channel; $b_b(x) + b_1(x)$ describes the change of the channel width at the level of water in the basin (e.g. figure 1b). The power m defines the behavior of the channel width with depth (e.g. figure 2a). If $m=1$, the width decreases linearly with depth (trapezoidal channel); $m=0$ and $m=\infty$ give rectangular sections. Note that the shape of the channel sides plays no role (Dalziel 1992, p. 1189). Only the distance between them, $b(x, z')$, matters (figure 1c; see equivalent figure 2.13 in Baines 1995).

We shall obtain analytical solutions for the channels with following cross-sections:

- a) Channels with similar sections: $b_b(x) = (1-a)b'(x)$, $b_1(x) = ab'(x)$;

b) Channel sections with $b_b(x)=b'(x)$, $b_1(x)=a$;

c) Geometry with trapezoidal sections which transform from triangular to rectangular: $b_b(x)=(1-x)^2/a$,
 $b_1(x)=x^2$; $m=1$, $h(x)=0$.

The width of these channels can be written in the following forms:

$$b(x,z')=b'(x)B(z/(H+h(x))), \quad (2.13a)$$

$$b(x,z')=b'(x)+B(z/(H+h(x))), \quad (2.13b)$$

$$b(x,z')=(1-x)^2/a+x^2(1-z/H). \quad (2.13c)$$

The first case gives an example when the left side of equation (2.2) has the form $F(x,\xi)=S'(x)f(\xi)$. Thus x_c and ξ_c can be found as positions of the minimum of $S'(x)$ and the maximum of $f(\xi)$. For the last two cases both equations (2.9) and (2.10) contain the unknowns x_c and ξ_c and the problem becomes more complicated. Therefore, the first attempt has to be made to approximate the channel geometry in the form (2.13a).

3. Channels with similar sections: $b(x,z')=b'(x)B(z')$

(a) General solution

If the channel section can be approximated in the form (2.13a), then the problem to find the critical point of a surface is reduced to the problem of finding the critical points of two curves. The system (2.9) and (2.10) separates into two independent equations:

$$s'(\xi_c)=2\xi_c B(\xi_c), \quad (3.1)$$

to find ξ_c , and

$$S'_x(x_c)=0 \quad (3.2)$$

to find x_c . Here

$$S'(x)=(H+h(x))^{3/2}b'(x) \quad (3.3)$$

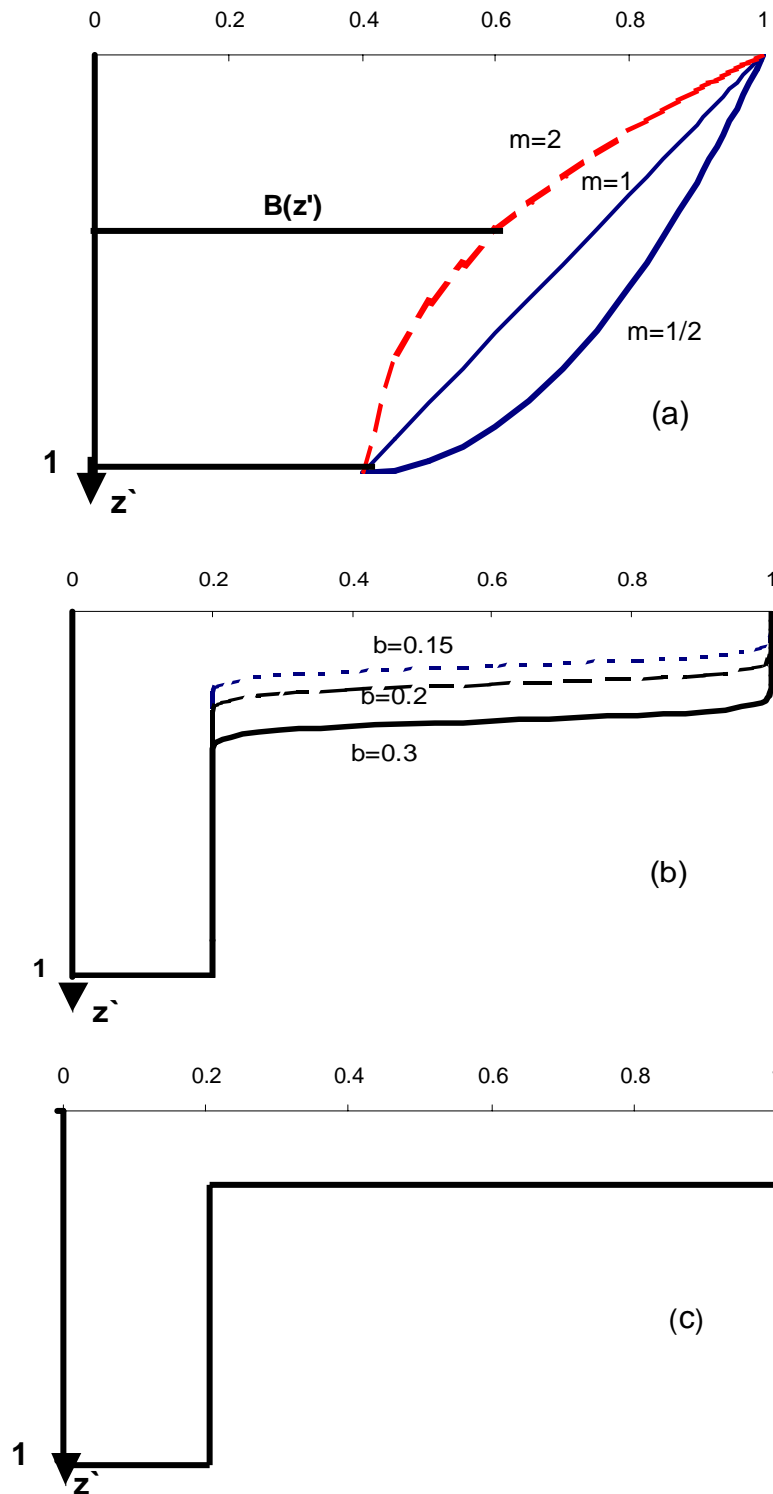


Figure 2. Channel section areas whose widths vary with depth as: (a) $B(z')=1-a+a(1-z')^m$ with $a=0.6$, and $m=1/2, 1, 2$. (b) $B(z')=1-a+a \tanh(40(z'-b))$ with $a=.4$ and $b=0.15, 0.2$ and 0.3 . (c) $B(z')=1$ for $0 < z' < 0.2$ and $B(z')=0.2$ for $0.2 < z' < 1$.

and

$$s'(\xi) = \int_{\xi}^1 B(z') dz' \quad (3.4)$$

The value of ξ_c depends only on the variation of B with z' . Mathematically, the problem to find ξ_c from (3.1) is identical to the problem to find the critical state of flow in a prismatic channel (Chow, 1959, § 3-3). To minimize the error due to the approximation, the channel width at the free surface and the flow cross-section area must be approximated accurately. The shape of the channel section at $\xi < 1/3$ never plays any role as long as the flow cross-section area stays the same. The position x_c depends only on the along channel geometry (the position of the minimum of $(H+h(x))^{3/2}b'(x)$). The problem to find the position of the critical section is the same for any channel section shape, in particular for a rectangular channel (Gill, 1977, § 2).

For channel geometry (2.13a) equation (2.6) takes the form

$$\xi^{1/2}s'(\xi) = (Q/(2g)^{1/2})/S'(x). \quad (3.5)$$

The left side of (3.5) is a function of ξ only. The right side of (3.5) is a function of x only. If the function $f(\xi) = \xi^{1/2}s'(\xi)$, $0 < \xi < 1$, has a unique maximum f_c , at $\xi = \xi_c$, (dash line in figure 3a), and the function $S'(x)$ has a unique minimum S'_c , at $x = x_c$, ($1/S'(x)$ is shown in figure 3b), then there is a unique discharge

$$Q = (2g)^{1/2} f_c S'_c, \quad (3.6)$$

for which equation (3.5) has a continuous solution $\xi(x)$ for all x such that: ξ increases from 0 to ξ_c , when $S'(x)$ decreases from ∞ to S'_c , upstream of x_c ; then ξ increases from ξ_c to 1, when $S'(x)$ increases from S'_c to ∞ , downstream of x_c (see figure 3a,b). All geometries with the same maximum of $f(\xi)$ and the same minimum of $S'(x)$ have the same discharge.

If $f(\xi)$ has more than one local maximum in the interval $0 < \xi < 1$ (figure 3c) and the function $S'(x)$ has a unique minimum S'_c , (as in figure 3b), then the continuous solution $\xi(x)$ of equation (3.5) is multi-valued.

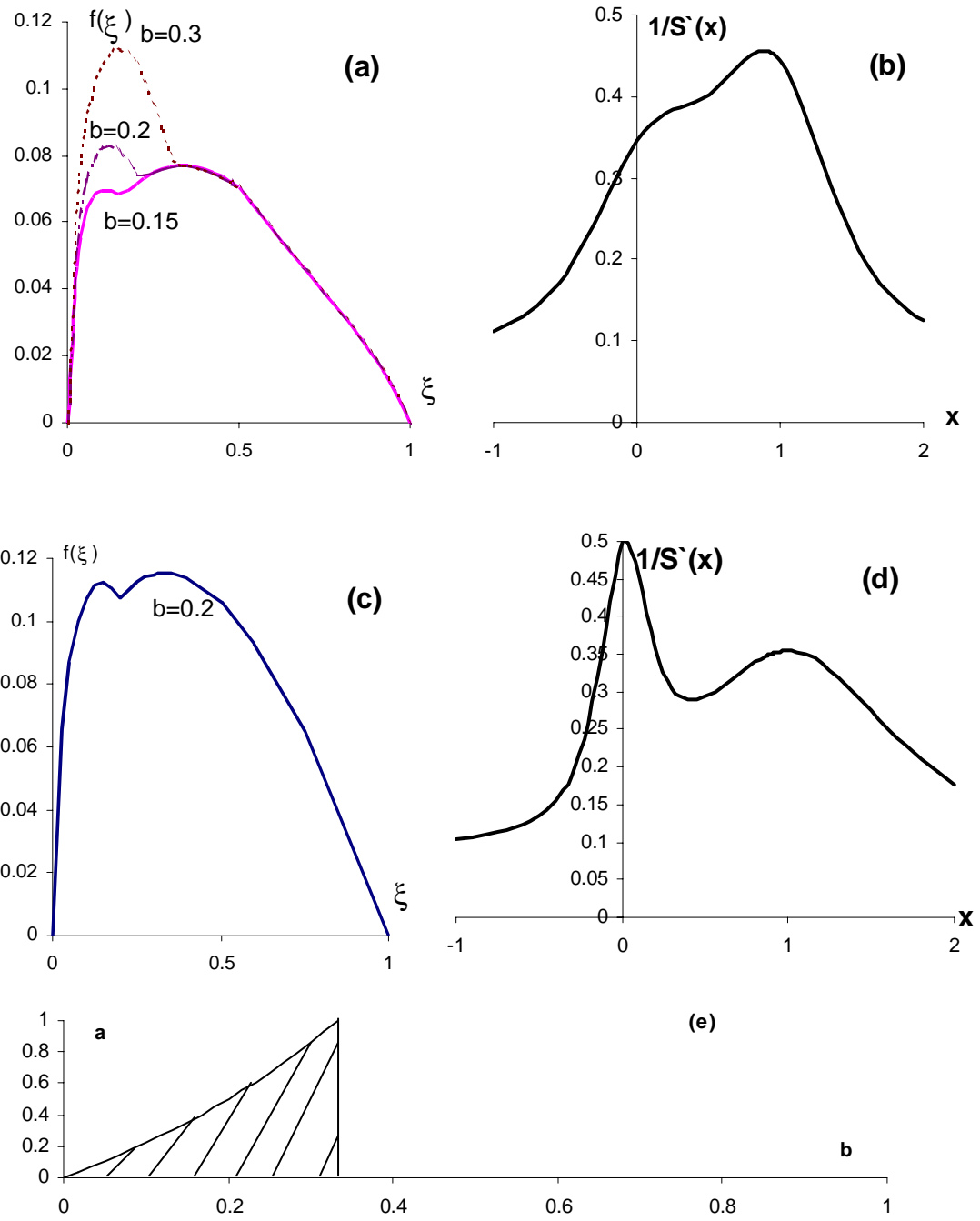


Figure 3. Graphs of $f(\xi)$ and $1/S'(x)$ (see (3.5)): (a) for the cross-section shown in figure 2(b); (b) for the channel geometry shown in figure 1a,b; (c) for the cross-section shown in figure 2(c); (d) for the channel geometry used by Helfrich (1995, Eq. (19)-(20)). (e) The area (shaded) of the parameters a and b for which a continuous solution of (3.5) does not exist for the channel section $B(z')=1$ for $0 < z' < b$ and $B(z')=a$ for $b < z' < 1$.

If $f(\xi)$ has a unique maximum and the function $S'(x)$ has several local minima, (as in figure 3d) then the continuous solution $\xi(x)$ of the equation (3.5) is non-monotonic. Experiments can resolve if this solution has a physical meaning.

In general, by drawing the functions $f(\xi)$ and $1/S'(x)$, one finds $f(\xi_c)$ and $S'(x_c)$ graphically.

(b) Analytical solution

Channel with parabolic cross section. Consider the channel section of the form (figure 2a)

$$B(z')=1-a+a(1-z')^m. \quad (3.7)$$

Here a and m are constants. In this case the solution $\xi_c(m,a)$ of (3.1) in the implicit form is

$$(1-a)/a=(1-\xi_c)^m(2m+3-1/\xi_c)/((m+1)(1/\xi_c-3)). \quad (3.8)$$

Let $0 < a < 1$ and $m > 0$. Then $\xi_c(m,a) \rightarrow 1/3$ when $m \rightarrow 0, \infty$ and $2m+3 > 1/\xi_c(m,a) > 3$. The graphs of the non-dimensional thickness of the flowing layer $\eta_c(m,a)/(H+h(x_c))=1-\xi_c(m,a)$ are shown in figure 4a (heavy lines).

The discharge is

$$Q(a,m)=Q_r(1-a)/(1-(1/\xi_c-3)/2m). \quad (3.9)$$

Or, alternatively,

$$Q(a,m)=Q_r 2am(1-\xi_c)^m/((1/\xi_c-3)(1+m)). \quad (3.10)$$

Here $Q_r(x_c, \xi_c)=(2g)^{1/2}S'(x_c)\xi_c^{1/2}(1-\xi_c)$ and ξ_c is determined by (3.8). The graphs of $q(a,m)=Q(a,m;x_c)/(2g)^{1/2}S'(x_c)$ vs. m and a are shown in figure 4b (heavy lines).

If a (or m) is zero (the rectangular section profile) then $\xi_c=1/3$ and $q(0,m)=q(a,0)=q_r \approx 0.3849$.

If $a=1$ (zero bottom width) then $\xi_c=1/(2m+3)$ and $q(1,m)=2[2(m+1)]^m/(2m+3)^{m+1.5}$ (in agreement with (24) in Dalziel (1992)). When m increases from 0 to infinity, the top width $B(\xi_c)$, the water surface drop ξ_c and the non-dimensional discharge q decrease from 1, $1/3$ and $2/27^{1/2}$ to $1/e^{1/2}$, 0 and 0, respectively. If $m=1$ (triangular channel section) we have $\xi_c(1,1)=1/5$ and $q(1,1)\approx 0.1431$.

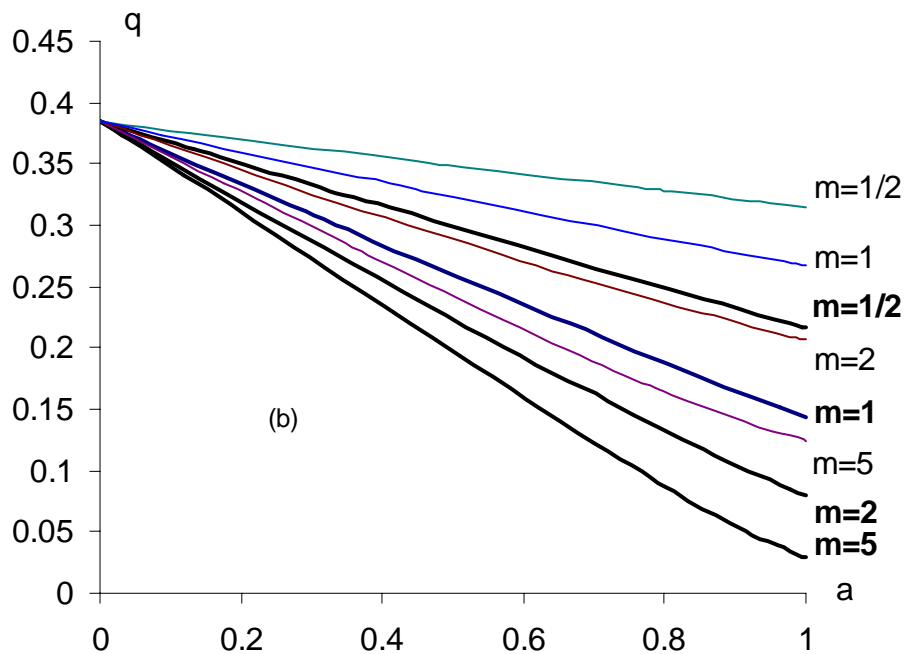
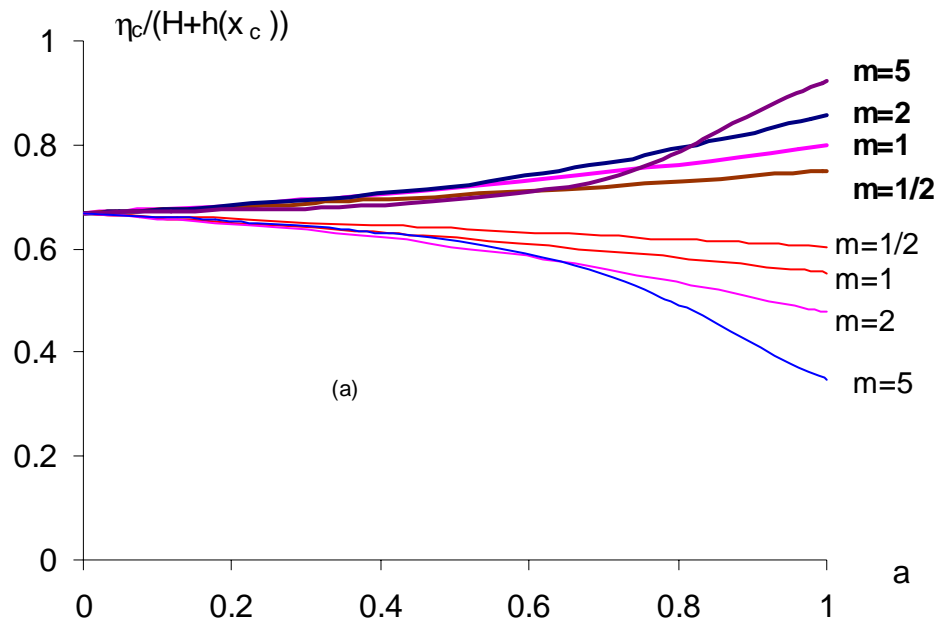


Figure 4. Graphs of (a) the thickness of the moving layer η_c and (b) the non-dimensional discharge q vs. a for the geometry $b(x, z) = b(x)[1 - a + a(1 - z)^m]$, $m=0.5, 1, 2, 5$. Heavy lines are for a withdrawal (see (3.8), (3.10)); light lines are for run up (see (A.6), (A.7)).

Calculations show (figure 4b), that $q(a, m)$ is almost a linear function of a and the approximate formula $q(a, m) \approx 0.3849[1 - C(m)a]$ can be used. Here

$$C(m)=1-[(m+1)/(m+1.5)]^m/(1+2m/3)^{1.5}. \quad (3.11)$$

In particular: $C(0)=0$, $C(1)\approx 0.6282$, $C(\infty)=1$. For a trapezoidal section, $m=1$, we have $\xi_c=(2-a)/(3+(4+5(1-a)^2)^{1/2})$ and $q=2(1-a)\xi_c^{3/2}(1-\xi_c)/(5\xi_c-1)\approx 0.3849(1-0.6282a)$.

Discussion. Larger a and/or m correspond to a smaller channel section area. Figure 4 shows that $q(a,m)$ is a decreasing function of a and m and $\eta_c(a,m)$ is a increasing function of a . But $\eta_c(a,m)$ is not a monotonic function of m . The relative water surface drop $\xi_c(a,m)$ (and as result the water velocity at the critical point, $u^2(x_c)=2g(H+h(x_c))\xi_c$), tends to the maximum value when $m\rightarrow 0,\infty$ and reaches the minimum for a certain value of $m(a)$.

Exponential along channel geometry. A wide family of along channel geometries can be approximated in the two-parametric ($\alpha>0$ and $c>0$ are arbitrary parameters) form

$$h(x)/H=-1+\exp[2\alpha cx^2/3], \quad b'(x)=\exp[c(1-x)^2]. \quad (3.12)$$

For this geometry (3.2) becomes the linear equation and the solution is $x_c=1/(1+\alpha)$. The parameter α characterizes how fast the depth changes with width ($\alpha=0$ corresponds to a pure contraction, $\alpha\rightarrow\infty$ corresponds to a pure sill). It illustrates that the critical point is closer to the crest if the width changes more slowly than the depth and vice versa.

Discussion. If the channel geometry can be approximated in the form $b(x,z')=b_0[1-a+a(1-z')^m]\exp[c(1-x)^2]$, $h(x)/H=\exp[2\alpha cx^2/3]-1$, $H z'=z\exp[-2\alpha cx^2/3]$, then the discharge is

$$Q\approx Q_r[1-C(m)a]\exp[c\alpha/(1+\alpha)]. \quad (3.13)$$

Here $Q_r=(8gH/27)^{1/2}Hb_0$ is the discharge through a rectangular section channel with the minimum width b_0 at the sill. Roughly speaking, the second term in (3.13) decreases the discharge due to the decrease of the cross-section; the last term in (3.13) increases the discharge due to the fact, that the sill and the narrows do not coincide. Their product could be close to 1, and usage of the incorrect formula $Q=Q_r$ can accidentally give a good result.

For geometry (3.12) with Q given by (3.6) we can solve (3.5) in implicit form

$$(1+\alpha)x=1-\alpha/2\pm[\alpha^2/4+((1+\alpha)/c)\ln(f(\xi_c)/f(\xi))]^{1/2}. \quad (3.14)$$

Here $f(\xi)$ is the left side of (3.5), signs \pm are for the flow upstream/downstream of x_c . For any $B'(z')$ one can draw the water surface profile $\xi(x)$ using (3.14).

(c) Examples of channel sections for which a solution does not exist

There are several examples of channel cross-sections, for which $f(\xi)$ has more than one local maximum in the interval $0 < \xi < 1$ (figure 3c and dash lines in figure 3a). If the function $S'(x)$ has a unique minimum S'_c , (as in figure 3b), then the continuous single-valued solution $\xi(x)$ does not exist.

The channel section with $B(z')=1$ for $0 < z' < b$ and $B(z')=a < 1$ for $b < z' < 1$ (figure 2c) gives an example of the geometry for which $f(\xi)$ has two local maxima (figure 3c) for a certain range of the parameters a and b (figure 3e). The solution of (3.1) can be easily found: $\xi_c=1/3$, $q=2a/27^{1/2}$ if $b < a/(2+a)$ and $\xi_c=(a+b-ab)/3$, $q=2[(a+b-ab)/3]^{3/2}$ if $b > 1/3$. Here $q=Q/(2g)^{1/2}S'(x_c)$. If $a/(2+a) < b < 1/3$ (shaded area on figure 3e) the continuous solution $\xi(x)$ does not exist.

Figure 2b shows other examples of the channel cross-sections, for which $f(\xi)$ has two maxima (figure 3a).

(d) The water surface profile

Parabolic cross-section. Substituting (2.11) into (2.6) gives the equation for the water surface profile $\xi(x)$

$$\xi^{1/2}s(x,\xi)(H+h(x))^{3/2}=F(x_c,\xi_c). \quad (3.15)$$

This equation does not contain g . This means that the shape of the free surface of the fluid flowing into an empty basin and the shape of the interface of the fluid flowing into a basin of lighter fluid with the same level are identical.

For a channel cross-section defined by (2.13a) and (3.7) the equation (3.15) gives

$$\xi^{1/2}(1-\xi)[1-a+a(1-\xi)^m/(m+1)]=qS'(x_c)/S'(x). \quad (3.16)$$

Here $q=2\xi_c^{3/2}[1-a+a(1-\xi_c)^m]$. Having x_c and ξ_c , we can calculate $\xi(x)$ from (3.16) and find the velocity $u(x)=[2g(H+h(x))\xi(x)]^{1/2}$. We can not solve (3.16) analytically for arbitrary a , m and $S'(x)$. We shall give an explicit solution for a rectangular profile channel and arbitrary $S'(x)$ to discuss the behavior of the water surface at the critical point.

Rectangular cross-section and arbitrary along channel geometry. For a rectangular profile ($a=0$, $q=2/27^{1/2}$) we can solve (3.16) explicitly

$$\xi(x)=(4/3)\sin^2\theta. \quad (3.17)$$

Here $\theta=(\arcsin \varphi(x))/3$ upstream of x_c , $\theta=(\pi-\arcsin \varphi(x))/3$ downstream of x_c and $\varphi(x)=S'(x_c)/S'(x)$. If $S'(x)$ has a unique minimum (figure 3b), (3.17) shows that $\xi(x)$ is a monotonic function, but $\zeta(x)$ can have several local extrema. An example of $\zeta=(H+h(x))\xi$ for the geometry $h(x)/H=\tanh^2(5x/4)$, $b(x)=4-3/e^{(1-x)^2}$ is shown in figure 1a.

For arbitrary along channel geometry $S'(x)$ we have from (3.17)

$$\xi_x(x)=(4/9) [|\varphi_x| / (1-\varphi^2)^{1/2}] \sin 2\theta. \quad (3.18)$$

In the neighborhood of x_c we can approximate

$$\varphi(x) \approx 1 - a_0 |x_c - x|^k \quad k > 1. \quad (3.19)$$

Here $a_0 > 0$ is a constant. This leads to $|\varphi_x(x)| \approx ka_0 |x_c - x|^{k-1}$ and $\xi_x(x) \sim |x_c - x|^{-1+k/2}$. Therefore $\xi_x(x_c)$ is zero if $k > 2$, is finite only if $k=2$ (see note after (3.4) in Gill (1977)) and is infinite if $1 < k < 2$. So the water surface slope at the critical point can be 0, finite or infinitely large.

Example. For the channel geometry $(1+h(x)/H)=(1+|x|)^{1/6}$ and $b(x)/b(0) = (1+|x|)^{1/4}$ we get $x_c=0$ and $\varphi(x)=(1+|x|)^{-1/2}$. Thus $|\varphi_x| / (1-\varphi^2)^{1/2} = 0.5kx^{-1+k/2} / (1+|x|)^k$ and $\xi_x(x) \sim x^{-1+k/2}$ for $x \rightarrow 0$. This is the example of geometry with $[1+h(x)/H]^3 = [b(x)/b(0)]^2$ (see § 3.2 in Odulo & Swanson, 1998).

(e) Dependence of the discharge on the fluid level in the basin

In this subsection we discuss how the discharge depends on the fluid level in the basin, H , when $h(x)$ and $b'(x)B(z')$ stay unchanged. If the sill and narrows coincide, then $x_c=0$ and the discharge $Q_0=(2g)^{1/2}f(\xi_c)b_0H^{3/2}$. For the rectangular section profile $B(z')=1$, $f(\xi_c)=2/27^{1/2}$. In this subsection we introduce the non-dimensional discharge as $q=Q/Q_0$.

The relation between x_c and H we find from (3.2)

$$H=-h(x_c)-1.5 b'(x_c)h_x(x_c) /b'_x(x_c) \quad (3.20)$$

We see that $x_c \rightarrow 0$ when $H \rightarrow 0$, and $x_c \rightarrow 1$ when $H \rightarrow \infty$. So for arbitrary $h(x)$ and $b'(x)$ we get the position of the critical point $x_c(H)$ from (3.20) and then the non-dimensional discharge $q(H)=(1+h(x_c)/H)^{3/2}b'(x_c)$. We see that $q \rightarrow b'(0)$ when $H \rightarrow 0$ and $q \rightarrow b'(1)$ when $H \rightarrow \infty$.

Example. We approximate the channel geometry by power functions: $h(x)=x^n$ and $b'(x)=1+(1-x)^k$, $n>1$, $k>1$. It is seen that $0<x_c<1$. The large n corresponds to the geometry with an almost flat bottom at the major part of the constriction and a rapidly increasing depth near the narrows. Similarly, the large k corresponds to geometry with almost uniform width at the major part of the constriction and a rapidly increasing width near the sill. The larger (smaller) the H the smaller (larger) the channel depth at the narrows compared with the water level in the basin. We get from (3.20) the expression for $x_c(H;k,n)$ in implicit form

$$H=[-x_c+1.5(n/k)(1-x_c)(1+1/(1-x_c)^k)]x_c^{n-1}. \quad (3.20)$$

The non-dimensional discharge is

$$q(H, k,n)=[1+x_c^n/H]^{3/2}[1+(1-x_c)^k]. \quad (3.21)$$

Discussion. We see that $q \rightarrow 1$ for large H and $q \rightarrow 2$ for $H \rightarrow 0$. For small H we have $H \approx (3n/k) x_c^{n-1}$. For small H and $n=2$ we see that $x_c(H)$ is linear function and $q(H,2,k) \approx 2(1-Hk^2/24)$. Figure 5 shows $x_c(H;k,n)$ and $q(H;k,n)$ vs. H for $(k,n) = (1.5,1.5), (4,1.25), (2,2), (2,4), (4,2)$ and $(4,4)$. The channel section areas at the crest and at the narrows are the same for the geometries considered (for any n and k). But channels with different section transformation between the crest and the narrows (different n and k) have significantly different discharge (figure 5). For example, $q(H,2,2)/q(H,4,4) \approx 3/2$ in interval $0.5<H<1$. Designing channels

with different along-channel geometries, one gets the constrictions with different withdrawal characteristics $q(H)$.

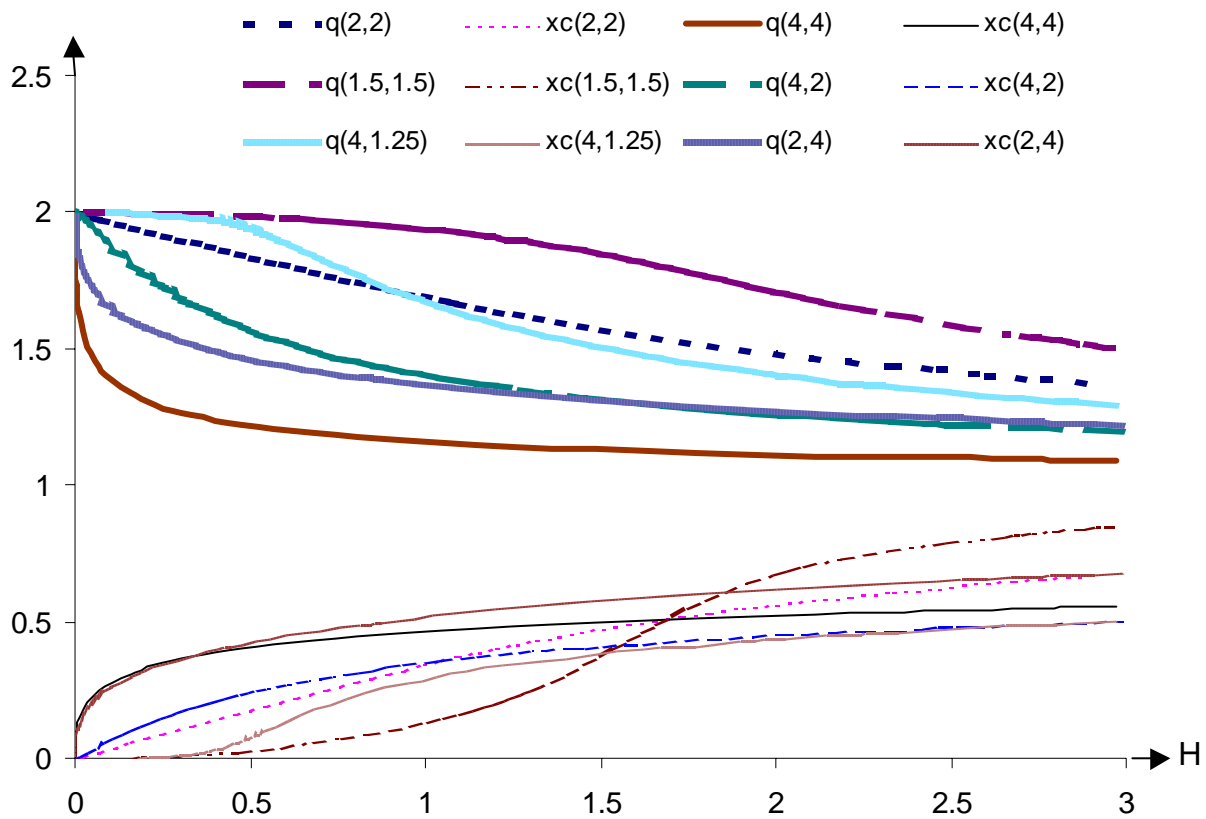


Figure 5 Graphs of the position of the critical point $x_c(H;k,n)$ (light lines) and the non-dimensional discharge $q(H;k,n)$ (heavy lines) vs. H for the geometry $h(x)=x^{2n}$ and $b'(x)=b_0(1+(1-x)^{2k})$ with $(k,n)= (1.5,1.5), (4,1.25), (2,2), (2,4), (4,2)$ and $(4,4)$.

Figure 5 shows that $q(H;k,n)$ can be approximated as linear functions of H at certain intervals, for example, $q(H,2,2) \approx 2-H/3$ for $0 < H < 1$. Such simple approximate formulae can be used to solve some unsteady problems, for example, to find the decrease of the water level of the emptying basin, $H(t)$, and the withdrawing discharge, $Q(t)$. Here t is time.

In the case of a withdrawal into a basin with a lighter fluid, changing of the level in the emptying basin will change not only H but also, more importantly, will change the difference between basin levels. If the

density difference is small, then a small change of the level difference leads to a significant difference of flow (Wood 1970, Odulo & Swanson 1998).

4. Channels with the cross-section $b(x,z')=b'(x)+B(z')$

Now we shall study the more complicated case of channel geometries with non-similar sections. To get an analytical solution we consider the channel geometries, which can be approximated in the form (2.13b). In (2.13b) the first term, $b'(x)$, describes the change of width along the channel. The second term, $B(z')$, describes the change of width with depth. Let $B(1)=0$, then $b'(x)$ is the bottom width.

(a) General solution

This geometry gives an example when the position of the critical point depends on both an along channel geometry and a cross-section shape. For geometry (2.13b) the system (2.9) and (2.10) becomes

$$(1-3\xi_c)b'(x_c)=2\xi_c B(\xi_c)-s'(\xi_c) \quad (4.1)$$

$$\gamma(x_c)=1+B_{av}(\xi_c)/b'(x_c) \quad (4.2)$$

Here $s'(\xi)=\int_{\xi}^1 B(z)dz$, $B_{av}(\xi_c)=s'(\xi)/(1-\xi_c)$, $\gamma(x)=-1.5b'h_x/[b'_x(H+h)]$. For a rectangular channel $B(z')=0$, so

(4.1)-(4.2) give $\xi_c=1/3$ and $\gamma=1$. Note that equation (3.2) can be written in the form $\gamma=1$.

We introduce $\lambda(x_c,\xi_c)=b'(x_c)/B(\xi_c)$ and $\mu(\xi_c)=B_{av}(\xi_c)/B(\xi_c)$. For the rectangular section profile $\mu=1$. If the channel width decreases with depth then $\mu<1$. We can rewrite (4.1) and (4.2) in the form

$$\xi_c=(\lambda+\mu)/(3\lambda+2+\mu), \quad (4.3)$$

$$(\gamma(x_c)-1)\lambda=\mu. \quad (4.4)$$

From (4.3) we see that $\xi_c=\mu/(2+\mu)$, when $\lambda=0$, and then increases and tends to $1/3$, when λ infinitely increases. For a parabolic cross section channel, $B(z')=B_0(1-z')^m$, we get $B_{av}(z')=B(z')/(m+1)$ and $\mu=1/(m+1)$.

Taking ξ_c from 0 to 1/3 one can solve the system (4.1)-(4.2) numerically for any $B(z')$.

(b) Parabolic cross section

If $B(z')=B_0(1-z')^m$, then (4.1)-(4.2) becomes

$$b'(x_c)/B_0=(1-\xi_c)^m(2m+3-1/\xi_c)/((m+1)(1/\xi_c-3)) \quad (4.5)$$

$$\gamma(x_c)=1-(1/\xi_c-3)/2m \quad (4.6)$$

Putting $b'(x_c)/B_0=(1-a)/a$ into (4.5) we get (3.8). From (4.5) we see that $3 < 1/\xi_c < 2m+3$. Using (2.11) and (2.12) we get

$$Q=Q_r/(1-(1/\xi_c-3)/2m) \quad (4.7)$$

Here $Q_r(x_c, \xi_c)=(2g)^{1/2}S'(x_c)\xi_c^{1/2}(1-\xi_c)$, $S'(x)=(H+h(x))^{3/2}b'(x)$; x_c and ξ_c must be found from the system (4.5)-(4.6).

Example. Consider the geometry with width decreasing linearly with depth and parabolically along a channel at $0 < x < 1$, $b(x, z')=(1-x)^{3n}/a+1-z'$, $n > 1/3$. Let $h(x)=Hx^2$. This is the geometry with a triangular section at the narrows, $x=1$, and a trapezoidal section elsewhere between $x=0$ and $x=1$. The channel width at the bottom is $(1-x)^{3n}/a$. The solution of (4.5)-(4.6) in implicit form is $(1-x_c)^{3n}=0.5a(1-\xi_c)(5-1/\xi_c)/(1/\xi_c-1)$, $1/\xi_c=5+(2/n)(1-x_c)x_c/(1+x_c^2)$. Introducing $q=Q/(2gH^3)^{1/2}$, we have $q=2\xi_c^{3/2}((1-x_c)^2/a+1-\xi_c)(1+x_c^2)^{3/2}$. When $a \rightarrow 0$ then $x_c \rightarrow 1$, $\xi_c \rightarrow 0.2$ and $q \rightarrow 0.64(.4)^{1/2}$. When $a \rightarrow \infty$ then $x_c \rightarrow 0$, $\xi_c \rightarrow 0.2$ and $q \rightarrow 0.32(.2)^{1/2}$.

Figure 6 shows graphs of $x_c(a)$, $\xi_c(a)$ and $q(a)$ for $n=0.375, 0.5, 1$ and 2 . Increasing a and/or n leads to decreasing cross section area, and, as a result, to decreasing q .

For $n=0.375$ and a certain range (between 1 and 1.3) of the parameter a , the surface $F(x, \xi)$ has three critical points. As result the graphs of $x_c(a)$, $\xi_c(a)$ and $q(a)$ are three-valued in this interval of the parameter

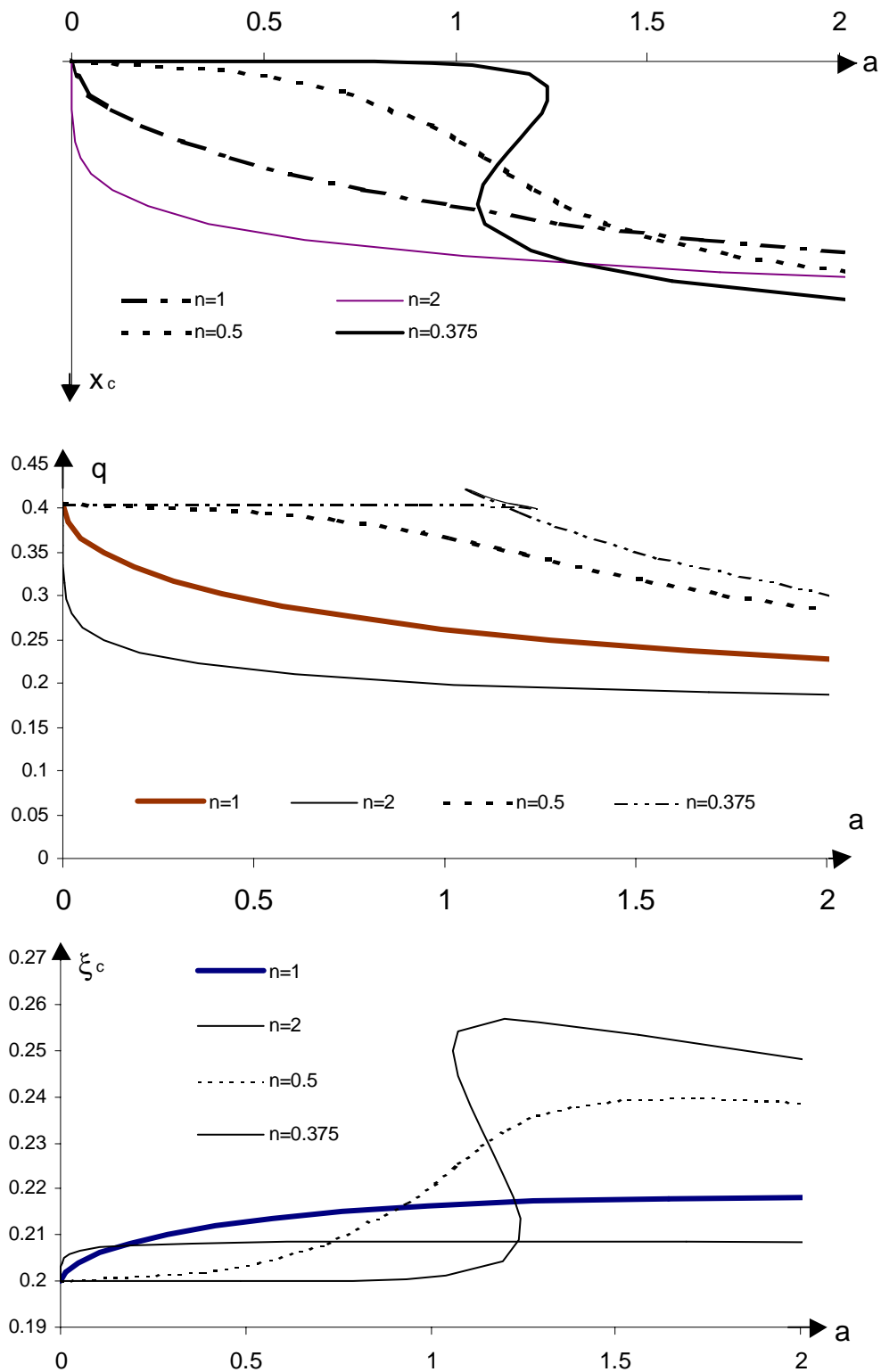


Figure 6. Graphs of x_c , ξ_c and q vs. the parameter a for a flow through a channel with geometry $b(x,z)=(1-x)^{3n}/a+1-z$ and $h(x)=Hx^2$ for $n=3/8, 1/2, 1$ and 2 .

5. Channels with trapezoidal cross-section $b(x,z)=(1-x)^2/a+x^2(1-z)$ and flat bottom,

$$h(x)=0$$

This geometry gives an example where the channel width at different depths has a minimum at different positions along the channel. The cross-section area is rectangular at $x=0$, with width equal to $1/a$, triangular

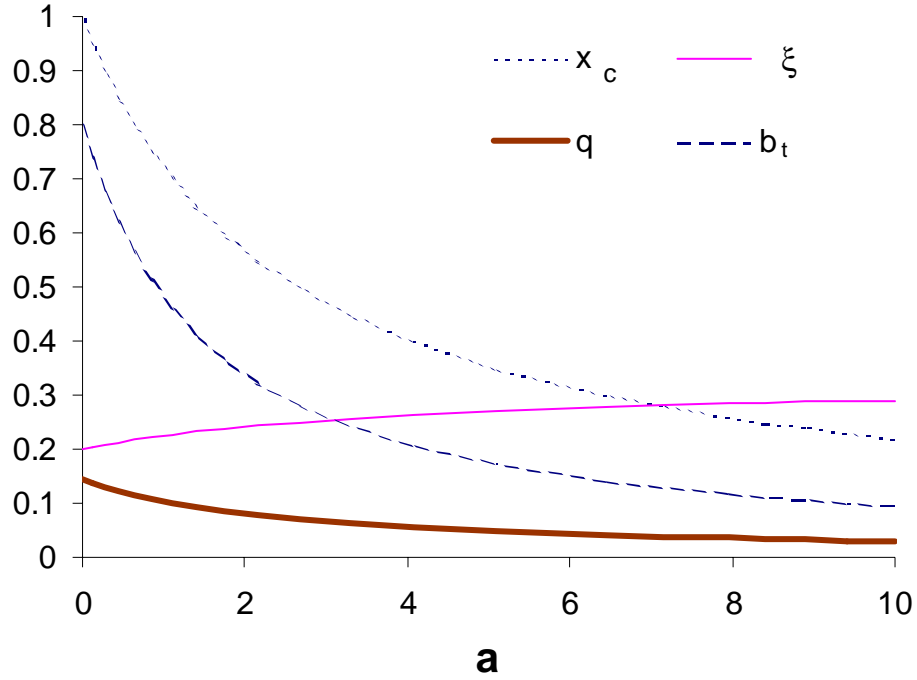


Figure 7. Graphs of x_c , q , ξ_c and b_t vs. a for the channel which section changes from rectangular at the crest to triangular at the narrows, $b(x,z)=(1-x)^2/a+x^2(1-z)$.

at $x=1$ and trapezoidal in between. At the bottom the position of the minimum width is always at $x=1$, $x_b(1)=1$, and the minimum width equals 0, $b(1,1)=0$. The top width b_t has a minimum at $x_b(\xi)=1/((1+a(1-\xi)))$ and equals $b(x_b(\xi),\xi)=(1-\xi)/(1+a(1-\xi))$. We see that $x_b(\xi)\rightarrow 0$ for large a and $x_b(\xi)\rightarrow 1$ for $a\rightarrow 0$. For this geometry, the equations (2.9), (2.10) and (2.11) yield

$$\xi_c=1/(3+2x_c), \quad (5.1)$$

$$a=(3+2x_c)(1-x_c)/x_c(1+x_c), \quad (5.2)$$

$$Q=(2gH^3)^{1/2}q, \quad q=\xi_c^{3/2}(1-\xi_c)x_c(1+x_c). \quad (5.3)$$

Solving the quadratic equation (5.2) one gets an explicit expression for $x_c(a)$. Substituting it into (5.1) and (5.3) one gets explicit expressions for $\xi_c(a)$ and $q(a)$.

When a increases from 0 to ∞ , x_c decreases from 1 to 0, ξ_c increases from 1/5 to 1/3, q decreases from 0.1431 to 0 and the top width $b(x_c, \xi_c)$ decreases from 0.8 to 0 (figure 7).

6. Plunging and run up

(a) Plunging or reduced gravity model

The result for withdrawal into an empty basin may also be applied to a two-fluid system when the lower denser (density ρ_1) layer is completely covered by the motionless lighter fluid (this requires that the free surface is flat) (figure 1a). Then in figure 1(a) the plane $z=0$ is the free surface, $z=\zeta(x)$ is the depth of the interface, the space between the free surface and the interface is filled by fluid density ρ_0 , and g must be replaced by the reduced gravity $g\varepsilon_0$ in the formulae. Here $\varepsilon_0=(\rho_1-\rho_0)/\rho_1$. This solution describes a flow, which separates the regime of exchange flow (which occurs when the level of lighter fluid is slightly higher than the level of denser fluid) from the regime when the plunge point is upstream of the critical point (which occurs when the level of denser fluid is slightly higher than the level of lighter fluid). See details in Odulo & Swanson (1998, § 2.1, figure 1e), where these regimes were called regimes 4 and 3, respectively (also see Wood 1970, § 2.2(a)).

(b) Run up on a rigid slope

The approach presented above can be applied to the problem of run up on a rigid slope. Let $h(x)$ monotonically increase from 0 at $x=-\infty$ to ∞ at $x=\infty$. This means that the sill is at $x=-\infty$ and $L=\infty$. Consider a flow from the infinitely deep basin. Let the channel width at the bottom be infinitely large far downstream. Then the free surface drop increases from 0 to H and the water velocity increases from 0 to $(2gH)^{1/2}$ in the flow direction from $x=\infty$ to $x=-\infty$. The critical point is downstream of the narrows and results obtained

above are valid in this case. In particular, solving the system (2.9)-(2.10) we find x_c , ζ_c and then Q from (2.11).

(c) Run up on a motionless layer of denser fluid

Consider again the channel geometry as described in the Introduction. But now, the basins are filled with fluids of different densities (ρ and $\rho_1 < \rho$), and the level of the lighter fluid is higher than the level of the denser fluid. Denote the difference of the levels in the basins as ζ_∞ . If ζ_∞ is large enough, the denser fluid is motionless (see details for rectangular section in Odulo & Swanson (1998), § 2.2). If in the area between the

$$\int_{\zeta_c}^{\zeta_c + (\zeta_\infty - \zeta_c)/\varepsilon} b_x(x_c, z) dz = 0 \quad (6.3)$$

the cross-section of flowing layer $S(x, \zeta) = \int_{\zeta}^{\zeta + (\zeta_\infty - \zeta)/\varepsilon} b(x, z) dz$ downstream of point x_p (see figure 8). Instead (2.9)

and (2.10) we get

$$S(x_c, \zeta_c) = 2\zeta_c(b_s - b_i + b_i/\varepsilon) \quad (6.2)$$

sill and the narrows, there is an interface with a motionless layer of denser fluid under it (figure 8), then we have $\zeta + \varepsilon\eta = \zeta_\infty$. Here η is the thickness of the flowing layer and $\varepsilon = (\rho - \rho_1)/\rho$ is the relative density difference.

The bottom profile under the motionless denser fluid has no influence on the discharge. In (2.2)

$$\zeta^{1/2} S(x, \zeta) = Q/(2g)^{1/2} \quad (6.1)$$

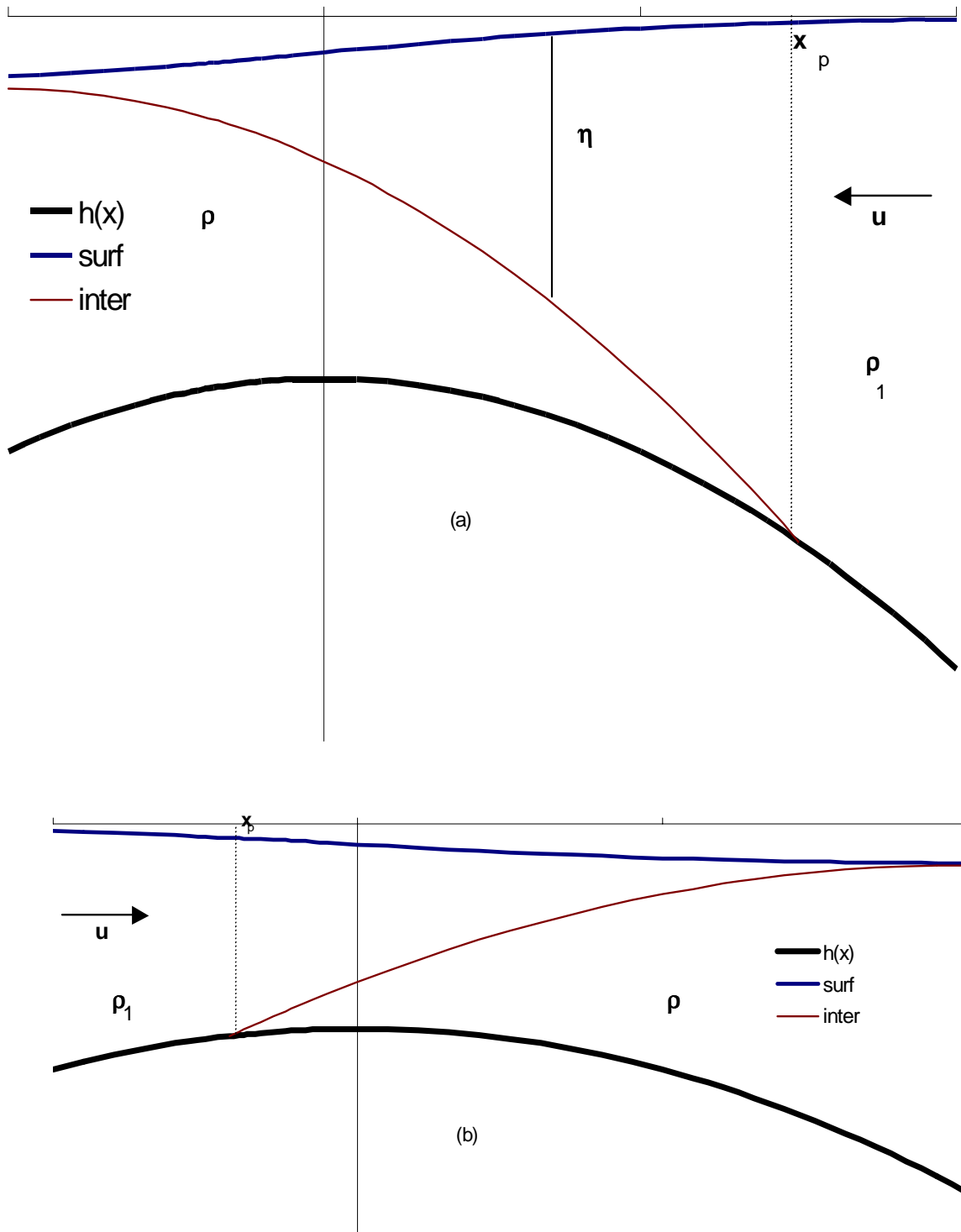


Figure 8. Sketch of run up on a motionless layer of denser fluid: (a) flow from a narrows to a sill; (b) flow from a sill to a narrows.

Here $b_s=b(x_c, \zeta_c)$ is the channel width at the free surface and $b_i=b(x_c, \zeta_c+(\zeta_\infty-\zeta_c)/\epsilon)$ is the channel width at the interface at the critical point. If we define the hydraulic depth as $D_i= S(x_c, \zeta_c)/[b_i+\epsilon(b_s-b_i)]$, then (6.2) can be written as $\epsilon D_i=2\zeta_c$ or $u^2(x_c)=g\epsilon D_i$.

For the channel with width $b(x,z)=b'(x)B(z)$ the solution of (6.3) is $x_c=x_b$. Here x_b is the position of the minimum of $b'(x)$. For a trapezoidal section $B(z)=1-az$, in the Boussinesq approximation ($\epsilon \ll 1$) the solution of (6.2) is

$$\eta_c=4\delta/[3+2a\delta+(9-8a\delta+4(a\delta)^2)^{1/2}] \quad (6.4)$$

Here $\eta_c=\delta-\zeta_c/\epsilon$ and $\delta=\zeta_\infty/\epsilon$. The discharge is

$$Q=(8g\epsilon\delta^3)^{1/2}(1-a\eta_c)b'(x_b). \quad (6.5)$$

This solution is valid as long as there is a motionless layer under the flowing layer at $x=x_b$. The value of $\delta=\zeta_\infty/\epsilon$, separating the exchange regime from that described above, depends on bottom topography. For a rectangular cross section, see the solution in Odulo & Swanson (1998, p. 53).

In the case of a flat bottom, this separating value is $\zeta_\infty/\epsilon=H$ (Appendix) for any $B(z)$. For a flat bottom and trapezoidal section, $B(z)=1-az$, the expressions (6.4) and (6.5) become $aH=(4-6\xi_c)/(4\xi_c-5\xi_c^2)$ and $q=Q/[2g\epsilon H^3 b'^2(x_b)]^{1/2}=2(1-\xi_c)^{1.5}(1-a\xi_c)$. Here $\xi_c=\eta_c/H$. Light lines for $m=1$ in figure 4 show $\xi_c(a)$ and $q(a)$.

(d) Moving layer surrounded by motionless layers

If the motionless denser fluid (density $\rho > \rho_1$) is everywhere under the moving layer then equation (6.1) is valid everywhere and the solution (6.2)-(6.5) can be used without any modification. Obviously, the shape of the bottom or the presence of layers of moving denser fluids beneath the motionless layer will have no influence on the motion of the layer density ρ_1 . In general, the presence of a motionless layer in n-layer flow decouples it: the dynamics of the fluid above the motionless layer have no influence on the motion of the fluid under the motionless layer and vice versa (see e. g. Engqvist 1996).

If, instead of a free surface, there is an interface between a moving layer and motionless lighter fluid (density $\rho_0 < \rho_1$), then we can use formulae (6.1)-(6.5) just replacing g with $g(\rho_1 - \rho_0)/\rho_1$ and ε with $(\rho - \rho_1)/(\rho - \rho_0)$.

7. Discussion

(a) Solution for one layer flow gives particular solutions for a multi-layer flow

For multi-layer flow, $n \geq 2$, the problem becomes more complicated. Similar to the one-layer problem, the discharges of all layers, Q_j , $j=1, \dots, n$, can be found from the condition that the thickness of each layer, $\eta_j(x)$, continuously decreases to 0 in the flow direction (Wood 1968, 1970, 1978; Wood & Lai 1972; Bryant & Wood 1976). For a given channel geometry and a given difference of the levels in the basin, ζ_∞ , the solution depends on $2(n-1)$ parameters, which are relative density differences $\varepsilon_{k,n}$, $k=1, 2, \dots, n-1$, ($\varepsilon_{m,j} = (\rho_j - \rho_m)/\rho_j$, $m < j$), and the non-dimensional thickness of each layer (except the lowest) far upstream from a constriction, $\xi_{ku} = \eta_{ku}/H$. Depending on relations between these parameters, different regimes are possible. For example, if k upper layers move in the same direction and

$$\zeta_\infty/H = \varepsilon_{1,k+1}\xi_{1u} + \varepsilon_{2,k+1}\xi_{2u} + \dots + \varepsilon_{k,k+1}\xi_{ku}, \quad (7.1)$$

then the layer of density ρ_{k+1} is motionless, $Q_{k+1}=0$; everywhere along a channel

$$\zeta + \varepsilon_{1,k}\eta_1 + \varepsilon_{2,k}\eta_2 + \dots + \varepsilon_{k,k+1}\eta_k = \zeta_\infty; \quad (7.2)$$

and the solution for the layers above and beneath the motionless layer can be found separately (Engqvist 1996). If the second from the bottom layer is motionless, $Q_{n-1}=0$, then the discharge of the lowest layer can be found as discussed in § 6a,b. If the second from the top layer is motionless, $Q_2=0$, then the discharge of the upper layer can be found as discussed in § 6c.

The result for one layer flow may also be applied to the cases when motionless layers above and below surround k layers moving in the same direction through a rectangular channel (for $k=2$ see figure 1 in Wood 1968). In this case the flow is self-similar

$$\eta_m(x)/\eta_{mu}=1-\zeta(x)/\zeta_\infty, \quad m=1, 2, \dots, k. \quad (7.3)$$

The problem can be reduced to one equation for $\zeta(x)$, which has the same form as for one layer flow. But the flow is not self-similar if instead of the lower interface there is a non-flat bottom (Wood & Lay 1972) or the channel section is non-rectangular.

(b) Definition of the critical point

In this paper we defined the critical point as a critical point of the function $F(x, \zeta)$, which is the left side of (2.2). The requirement that ζ continuously changes from 0 upstream to $H+h(x)$ far downstream leads to the unique solution with discharge $Q=(2g)^{1/2}F(x_c, \zeta_c)$, see (2.4).

Considering n -layer flow (Bryant & Wood 1976, pp. 586-587), we can take $\zeta_\infty=0$ without losing generality; a free surface case corresponds to $\rho_1=0$ and $\xi_{1u}=\zeta_\infty$. The expression for the free surface slope can be found from the momentum and continuity equations

$$\zeta_x = D_0(x; Q_j, \xi_{ku}, \epsilon_{k,n})/D(x; Q_j, \xi_{ku}, \epsilon_{k,n}). \quad (7.4)$$

The requirement that both the numerator and the denominator of this expression are zero at the same points x_i ($i=1, 2 \dots n$) (Bryant & Wood 1976, pp. 586-587 called them the “critical points”, x_{ic}), gives $2n$ relations

$$D_0(x_{ic}; Q_j, \xi_{ku}, \epsilon_{k,n})=0, \quad (7.5)$$

$$D(x_{ic}; Q_j, \xi_{ku}, \epsilon_{k,n})=0. \quad (7.6)$$

See example for $n=3$ in Smeed (2000). Excluding x_{ic} one gets n relations $G_j(Q_j, \xi_{ku}, \epsilon_{k,n})=0$ to find Q_j for given ξ_{ku} and $\epsilon_{k,n}$.

For a layer density ρ_1 flowing between motionless layers density ρ_0 and ρ ($\rho_0 < \rho_1 < \rho$) instead (1.2) and (6.2) we have

$$u^2=2g(\rho_1-\rho_0)\zeta/\rho_1 \quad (7.7)$$

and

$$S(x_c, \zeta_c)=2\zeta_c(b_s+(\rho_1-\rho_0)b_i/(\rho-\rho_1)) \quad (7.8)$$

Here $b_s=b(x_c, \zeta_c)$ and $b_i=b(x_c, \zeta_c+(\zeta_\infty-\zeta_c)(\rho-\rho_0)/(\rho-\rho_1))$ are the channel width at upper and lower interfaces at the critical point, respectively. Obviously, we can define the hydraulic depth, D_{si} , and the local Froude number, $Fr(x)$, in a such way that $Fr(x_c)=1: D_{si}=S(x, \zeta)/[b_s+(\rho_1-\rho_0)b_i/(\rho-\rho_1)]$ and $Fr^2(x)=u^2/[D_{si}g(\rho_1-\rho_0)/\rho_1]$. Calling the velocity at the critical point the critical velocity, $u_c^2= D_{si}g(\rho_1-\rho_0)/\rho_1$, one can call the flow upstream of the critical point sub-critical, and downstream of the critical point super-critical.

(c) Concluding remarks

To determine the discharge of the withdrawing fluid from a large basin one has to find the value of the function $F(x, \xi)$ at the saddle point. It can be found numerically remembering that x_c is between a bottom crest and a narrows and $\xi_c < 1/3$. Analytically $F(x_c, \xi_c)$ can be found for some particular geometries.

The analytical solutions presented in this paper demonstrate the influence of the channel geometry on the discharge. The geometries, considered above, contain the parameters a , k , m and n . These parameters characterize the behavior of the width and depth along the channel. When these parameters change in a such way that the channel cross-section increases, then the discharge always increases, but the water surface drop (and therefore the velocity) at the critical point can increase or decrease (see figures 4, 6,7). Clearly, the general formula which practicing engineers could use for discharge calculations does not exist. However, for some classes of geometries, the approximation formulae can be found. For example, for channels, which geometry can be approximated in the form (2.13a) with cross-section (3.7) and along channel geometry (3.12), the approximation formula (3.13) can be used.

Nomenclature

a, k, m and n	arbitrary numbers;
$b(x, z')$	channel width;
$D(x, \zeta)$	hydraulic depth of water area;
$f(\xi)$	the left side of (3.5) ($=\xi^{1/2}s'(\xi)$);

ε	relative density difference $(=\rho-\rho_1)/\rho$;
g	gravitational constant;
H	the water surface level in the basin measured from the bottom crest datum;
$h(x)$	depth of the lowest point of the channel section measured from the bottom crest level;
L	distance between the bottom crest and the narrows;
$s(x,\xi)$	$= S(x,\zeta)/(H+h(x))$;
$S(x,\zeta)$	fluid cross-section area (see (2.1));
$S''(x,z')$	$=(H+h(x))^{3/2}b(x,z')$;
$S'(x)$	$=(H+h(x))^{3/2}b'(x)$;
q	non-dimensional discharge;
Q	discharge;
$u(x)$	mean flow velocity;
x	axis pointing along the channel from the bottom crest to the narrows;
z	axis pointing vertically downwards;
z'	$=z/(H+h(x))$;
ξ	relative water surface drop $(=\zeta/(H+h(x)))$;
$\zeta(x)$	water surface drop.

Subscripts

c	at critical point;
x	partial derivative over x ;
ξ	partial derivative over ξ .

Appendix. Exchange flow through a non-rectangular contraction

In this Appendix we show that the same method can be used to find the exchange flow through a non-rectangular section contraction.

Consider an exchange flow through a channel with variable width $b(x)B(z/H)$ and flat bottom in the Boussinesq approximation ($b(x)$ has a unique minimum at $x=0$ and infinitely increases at $x \rightarrow \pm\infty$). From the Bernoulli and continuity equations (Baines 1995, § 3.10) we get the equation for the non-dimensional interface depth (the thickness of the upper layer $\eta(x)=H\xi(x)$)

$$\varepsilon\delta + Q^2/(2gH^3b^2s^2) = \varepsilon\xi + Q_1^2/(2gH^3b^2s_1^2). \quad (\text{A.1})$$

Here $\delta = \zeta_\infty / \varepsilon H$ is a non-dimensional difference of the levels in the basins, H is the depth in the lighter basin far from the contraction, $\varepsilon = (\rho - \rho_1) / \rho$, ρ_1 and ρ are the densities of the upper and lower layers, Q_1 and Q are the discharges of the upper and lower layers and

$$s_1(\xi) = \int_0^\xi B(z') dz', \quad s(\xi) = \int_\xi^1 B(z') dz' \quad (\text{A.2})$$

are the fluid sections of the upper and lower layers. Because $\xi(x)$ changes from 0 upstream to 1 downstream, for $1 > \delta > 0$ we have that at some point $\xi = \delta$. Then from (A.1) we have

$$Q_1 = Q s_1(\delta) / s(\delta). \quad (\text{A.3})$$

If the width decreases with the depth, then $Q_1/Q > \delta/(1-\delta)$. From (A.2) and (A.3) it follows that $Q_1=0$ when $\delta=0$ and $Q=0$ when $\delta=1$. In the first case (A.1) becomes

$$\xi^{1/2} s(\xi) = q / b^*(x). \quad (\text{A.4})$$

Here $q = Q/Q^*$, $Q^* = (2\varepsilon g H^3)^{1/2} b(0)$, $b^*(x) = b(x)/b(0)$. In the second case (A.1) becomes

$$(1-\xi)^{1/2} s_1 = q_1 / b^*(x). \quad (\text{A.5})$$

Here $q_1 = Q_1/Q^*$. For rectangular channel $s = 1 - \xi$, $s_1 = \xi$ and we have $q = 2/27^{1/2}$, $\xi_c = 1/3$ for $\delta=0$ and $q_1 = 2/27^{1/2}$, $\xi_c = 2/3$ for $\delta=1$.

Consider the parabolic section (3.7). We already have the solution for $\delta=0$. For $\delta=1$, searching for the maximum of the function $(1-\xi)^{1/2}s_1$, we get $\xi_c(a,m)$ in an explicit form

$$1/a=1+((2m+3)(1-\xi_c)^{m+1}-1)/((m+1)(3\xi_c-2)) \quad (\text{A.6})$$

and non-dimensional discharge

$$q_1=2(1-\xi_c)^{3/2}(1-a+a(1-\xi_c)^m) \quad (\text{A.7})$$

(see light lines in figure 4). For $a=1$ we have $\xi_c=1-1/(2m+3)^{1/(m+1)}$ and $q_1=2/((2m+3)^{1/(m+1)})^{3/2+m}$ in agreement with (24) in Dalziel (1992). For $m=1$ we have $\xi_c=4/(3+2a+(5+4(1-a)^2)^{1/2})$ and $q_1=(1-\xi_c)^{1/2}\xi_c(1-a\xi_c/2)$.

From (A.3) we have that $Q_1=Q$ when δ satisfies the equation

$$s_1(\delta_-)=s(\delta_-). \quad (\text{A.8})$$

For a rectangular cross section $\delta_-=1/2$. If the channel width decreases with depth then $\delta_-<1/2$. The faster the width decreases with depth the smaller δ_- becomes. For a parabolic cross-section (3.7) the solution of (A.8) is $1/a=1-(2(1-\delta_-)^{m+1}-1)/((m+1)(1-2\delta_-))$. For $a=1$ we have $\delta_-=1-(1/2)^{1/(m+1)}$. For $m=1$ we have $\delta_-=(2-a)/(2+(2+2(1-a)^2)^{1/2})$.

Substituting (A.3) into (A.1) we get

$$s(\xi)(\xi-\delta)^{1/2}/[(s^2(\delta)/s_1^2(\delta)-s^2(\xi)/s_1^2(\xi))]^{1/2}=q_1/b'(x). \quad (\text{A.9})$$

If the left side of this equation, which we denote $f(\xi,\delta)$, has a unique maximum, then $\xi_c(\delta)$ can be found from the equation $f_\xi(\xi,\delta)=0$. Then we get the discharge $q_1(\delta)=f(\xi_c,\delta)$. Odulo *at al.* (1997a) obtained the analytical solution for the channel with a rectangular cross section. For arbitrary $B(z)$ the maximum of $f(\xi,\delta)$ can be found simply plotting $f(\xi,\delta)$ for given δ and $0<\xi<1$.

In particular, for $\delta=\delta_-$ (A.9) becomes

$$s(\xi)s_1(\xi)[(\xi-\delta_-)/((s_1(\xi)-s(\xi))s(0))]^{1/2}=q(\delta_-)/b'(x). \quad (\text{A.10})$$

For the triangular section, $B(z)=1-z$, we get $\xi_c\approx 0.3175$ and $q_1=q\approx 0.0745$. These values are less than the corresponding values for the rectangular section $\xi_c=.5$ and $q_1=q\approx 0.1768$.

For the channel cross-section $b(x,z/H)=.5b(x)/(z/H)^{1/2}$ we get $\delta_-=1/4$ and (A.10) becomes

$$(1+2\xi^{1/2})^{1/2}(\xi^{1/2}-\xi)=2q/b(x). \quad (\text{A.11})$$

From (A.4), (A.5) and (A.11) we get $\xi_c=1/4$, $q=1/4$ for $\delta=0$; $\xi_c\approx 0.31165$, $q=q_1\approx 0.1793$ for $\delta=1/4$; and $\xi_c=.5$, $q_1=.5$ for $\delta=1$. Comparing these numbers with corresponding values for rectangular and triangular profiles one can see the strong influence of the shape of the channel section on the discharge.

References

- Ackers P., White, W.R., Perkins, J.A., and Harrison, A.J.M. 1978 *Weirs and flumes for flow measurement*. John Wiley & Sons, NY, p. 327.
- Baines, P.G. 1995 *Topographic effects in stratified flows*. Cambridge University Press, NY, p. 481.
- Bakhmeteff, B. A. 1932 *Hydraulics of Open Channels*. McGraw-Hill Book Company, Inc., NY, p. 329.
- Bormans, M. and Garrett, C. 1989 The effects of nonrectangular cross-section on the exchange through the Strait of Gibraltar. *J. Phys. Oceanogr.* **19**, 1543-1557.
- Bryant, P. J. & Wood, I. R. 1976 Selective withdrawal from a layered fluid. *J. Fluid Mech.* **77**, 581-591.
- Chow, V. T. 1959 *Open-channel hydraulics*. McGraw-Hill Book Co., Inc. New York, N.Y.
- Dalziel, S.B. 1992 Maximal exchange in channels with nonrectangular cross-section. *J. Phys. Oceanogr.* **22**, 1188-1206.
- Engqvist, A. 1996 Self-similar multi-layer flow through a contraction. *J. Fluid Mech.* **328**, 49-66.
- Gill, A.E. 1977 The hydraulics of rotating-channel flow. *J. Fluid Mech.* **80**, 641-671.
- Helfrich, K. 1995 Time-dependent two-layer hydraulic exchange flows. *J. Phys. Oceanogr.* **25**, 359-373.
- Odulo, A.B. & Swanson, J.C. 1998 The steady flow between reservoirs with different density and level through a rectangular channel section of varying depth and width. *DAO.* **28**, **2**, 39-61.
- Odulo, A.B., Swanson, J.C. & Mendelsohn, D.L. 1997a The steady flow between reservoirs with different density and level through a contraction. *J. Mar.Res.* **55**, 31-55.
- Odulo, A.B., Swanson, J.C. & Mendelsohn, D.L. 1997b The steady flow between reservoirs with different density and level over a sill. *Cont. Shelf Res.* **17**, **13**, 1561-1580.

- Ohtsu, I., Yasuda, Y. & Hashiba, H. 1996 Incipient jump conditions for flows over a vertical sill. *Journal of Hydraulic Engineering*, ASCE **122**, **8**, 465-469.
- Pawlak, G. & Armi, L. 1997 Hydraulics of two-layer arrested wedge flow. *Journal of Hydraulic Research*. **35**, 603-618.
- Smeed D.A. 2000 Hydraulic control in 3-layer exchange flows: application to the Bab al Mandab. *J. Phys. Oceanogr.* **30**, 2574-2588.
- Wood, I.R. 1968 Selective withdrawal from a stably stratified fluid. *J. Fluid Mech.* **32**, 209-223.
- Wood, I.R. 1970 A lock exchange flow *J. Fluid Mech.* **42**, 671-687
- Wood, I.R. 1978 Selective withdrawal from two-layer fluid. *Journal of the Hydraulics Division*, ASCE **104**, **12**, 1647-1659.
- Wood, I.R. and Lai, K.K. (1972). "Flow of layered fluid over crested weir." *Journal of the Hydraulics Division*, ASCE, **98**, 87-104.

Short title: Withdrawal through a constriction